

THE CARBONISATION OF ANTHRACENE AND BIPHENYL UNDER PRESSURES OF 300 MNm^{-2} (3 kbar)*

H. MARSH,† F. DACHILLE,‡ J. MELVIN§ and P. L. WALKER, Jr.

Department of Material Sciences, Pennsylvania State University, University Park, Pennsylvania, 16802, U.S.A.

(Received 21 July 1970)

Abstract—Anthracene, biphenyl and selected mixtures have been carbonised to a maximum temp. of 600°C . under pressures approaching 300 MNm^{-2} (3 kbar) whilst sealed in gold tubes and contained within a hydrothermal pressure bomb. Resultant carbons were analysed by Stereoscan microscopy, mass spectrometry, X-ray diffraction techniques and optical microscopy. The carbons were graphitised at 2000° and 2800°C and examined. A new phenomenon was observed, namely the formation of a spherulitic (botryoidal) carbon, about μ -sized, which although intrinsically anisotropic can confer isotropic properties to the bulk graphite. These spheres are essentially the mesophase, the effect of pressure being to prevent their coalescence. Pressure enhances the graphitisability of the carbons. The addition of biphenyl reduces the graphitisability of the carbonised anthracene, but a mechanism involving co-condensation of biphenyl and anthracene molecules is not considered to be invoked, rather a dilution of the anthracene, thus preventing mesophase growth.

1. INTRODUCTION

Understanding of the phenomenon of graphitisability in soft carbons has been considerably enhanced by the studies of Brooks and Taylor[1] into the development and properties of the mesophase. The growth of these mesophase spheres in the isotropic fused state of the carbonised pitch, or pure organic compound is essentially a physical process, i.e. the growth of nematic

liquid crystals[2]. Honda *et al.*[3] supplemented the findings of Brooks and Taylor by examining in greater detail, the effect of temperature and soaking time upon growth and physical properties of mesophase, and finding that temperature and time were essentially complementary factors. As yet, the effect of pressure upon mesophase growth has not been examined and this study reports an initial survey.

There is some evidence to support initial predictions that pressure is a significant parameter. The physical growth of the mesophase depends ultimately upon the chemical formation of large aromatic molecules which constitute the essential packing units of the mesophase. Chemical equilibria and reaction rates may be critically dependent upon pressure[4], the effect of which, in carbonisation systems at a given temperature is to promote the formation of the necessary condensed aromatic molecules. By necessity,

*This study was undertaken by H. Marsh, initially at Pennsylvania State University, U.S.A., during the summer of 1969, and subsequently completed at Newcastle University, England.

†Northern Coke Research Laboratory, School of Chemistry, University of Newcastle upon Tyne, NE1 7RU, England.

‡Materials Research Laboratory, Pennsylvania State University, Pennsylvania 16802, U.S.A.

§Department of Geology, University of Newcastle upon Tyne, NE1 7RU, England.

a pressurised system must be isolated, preventing volatile evolution and hence molecular fragmentation. In carbonisation systems operating at one atmosphere, much of the molecular stacking order following coalescence of the mesophase is lost by disruption arising from such volatile evolution through the still plastic state of the system. It is well documented that pressure increases the viscosity of liquids, e.g. Grist, Webb and Schiessher [5] report an increase of viscosity (in a substituted tetrahydronaphthacene) by two orders of magnitude over a pressure range up to 200 MNm^{-2} (2 kbar). Thus, the effect of pressure will not only reduce considerably any tendency to bubble formation, but also reduce disorder produced by convection currents within the system (because of enhanced viscosity).

Choice of material to be carbonised was restricted to anthracene and biphenyl. This was because of the considerable detailed knowledge now available of the chemistry of carbonisation of these materials. Evans and Marsh [6, 7] completed a study of the carbonisation of pure aromatic materials, and mixtures thereof, the products of carbonisation being analysed in a mass spectrometer, whilst Walker and Weintraub [8] examined, by several techniques, the carbonisation of anthracene-biphenyl, and phenanthrene-biphenyl systems. The findings of these two studies formed a basis for the interpretation of the results of this study.

In the study of Evans and Marsh, single components or mixtures were carbonised in sealed silica ampoules under conditions somewhat comparable to those of Walker and Weintraub. Materials, carbonised singly or in two-component systems included acenaphthylene, anthracene, chrysene, pyrene, fluoroanthene, and phenanthrene. Products of carbonisation were analysed in a MS9 mass spectrometer. The aim was the identification of the products of carbonisation to develop a model of structure in low-temperature carbons which uses, as 'building-bricks', the mole-

cular structures identified in the analysis. One salient and relevant conclusion of the study was that no evidence was found for reactions occurring between the individual components of a mixture or their major products of pyrolysis. This non-interaction of the mixture components was attributed, partially, to the lack of coincidence of temperatures of maximum standing-concentrations of free radicals from respective components. It must therefore not be assumed that components of mixtures of aromatic molecules (as in coal and petroleum pitches) exhibit comparable chemical reactivities.

The study of Walker and Weintraub had a somewhat different objective. They attempted to control the degree of graphitizability of anthracene and phenanthrene by addition of biphenyl (a non-graphitising material). The effect of addition of biphenyl to the phenanthrene produced a greater decrease in graphitizability than comparable addition to anthracene. Photomicrographs of the carbons of the anthracene-biphenyl system indicated the simultaneous production of three distinct phases, attributed to anthracene, biphenyl and the binary system. However, in the carbonisation of phenanthrene-biphenyl mixtures, three phases of carbon structure could also be identified, but they were not produced simultaneously—each carbonised system had a homogeneous composition, the nature of the phase depending upon the composition of the initial mixture. Walker and Weintraub postulate that, due to the much greater reactivity of anthracene to that of phenanthrene or biphenyl, the carbonisation of anthracene-biphenyl mixtures will proceed initially via anthracene-anthracene condensation to give one phase (appearance of delayed coke), then via anthracene-biphenyl condensation (e.g. 4-(9-anthryl)-1-phenyl benzene) to form a second phase with the biphenyl-biphenyl condensation occurring last to form the third phase. However, phenanthrene and biphenyl have more comparable reactivities,

and as such, co-condensation occurs continuously.

In the pressurised experiments reported below it was considered opportune to examine, not only anthracene but also the anthracene–biphenyl system, in terms of graphitisability, chemical composition, physical appearance and anisotropy interrelating, if possible, the initially described predictions and the above findings. In addition an anthracene-SP-1 fines mixture and an anthracene–ferrocene mixture were carbonised, the former because of possible nucleation of the mesophase by small graphite crystals and the second because of the known action of iron as a graphitisation catalyst [9–11].

2. EXPERIMENTAL

The pressurised carbonisation apparatus is outlined in Fig. 1. A hydraulic compressor, actuated by compressed air, could transmit (via water) maximum pressures of 400 MN m^{-2} (4 kbars) to the high tensile-strength, Stellite 25 bombs. Taps could isolate the bombs during carbonisation runs and provision was made for release to the atmosphere. The anthracene, or mixtures with biphenyl, ferrocene and SP-1 fines (a spectroscopic grade of graphite from the Carbon Products Division, Union Carbide) were sealed in gold tubes and these tubes placed into the bombs, the latter were filled with distilled water and

connected to the pressurised manifold. Heating was at the rate of $0.5^\circ\text{C min}^{-1}$ to the final temperature with a ten minutes soaking time, except in two experiments when the soaking time was 16 hr and 18 hr (samples P11 and P12, Table 1). Split-tube electrical furnaces were raised to and lowered from the bombs. Rapid quenching in cold water was carried out at the end of a carbonisation. Gold tubing was used because of its chemical inertness, its malleability allowing the hydrothermal pressure to be transmitted directly on the specimen and because of ease of sealing. An arc welding technique provided a seal perhaps stronger than the walls of the gold tubing. No detectable weight loss from the sealed, gold tubes occurred during the carbonisation process. About 1.0 g of material was carbonised. The details of the experiments, with code number, are listed in Table 1. Here, the code numbers proceed in terms of pressure and temperature. Several techniques were used to examine the carbonised samples as removed from the gold tubes.

2.1 Description of original and graphitised samples

The physical appearance, colour, hardness etc., of the samples as taken from the gold tubes and after further heat-treatment, were recorded.

2.2 Stereoscan micrographs

Topographical features were revealed using a 'Stereoscan' (Cambridge Instrument Co., U.K.) scanning electron microscope [12]. A small sample, about 1 mm cube, was mounted on the mushroom-shaped specimen holder of the instrument, shadowed with gold-palladium alloy in high vacuum [13] to promote electrical conductivity and examined at magnifications up to $2000\times$.

2.3 Mass spectrometric analysis

The chemical composition of the carbonised product was determined using an MS9

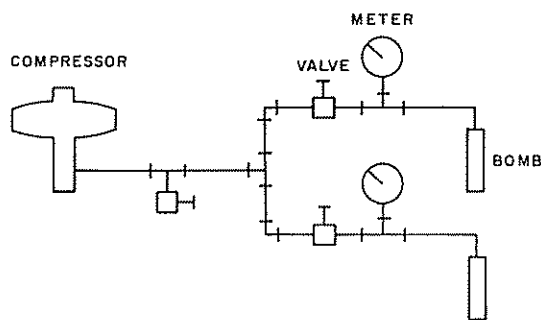


Fig. 1. Diagram of pressurised carbonisation apparatus.

Table 1. Description of sample preparation

Code	Composition of sample	HTT °C	Soak time (min)	Pressure		
				MNm ⁻²	kbar	p.s.i.
P1	Anthracene	500	10	13	0.13	2000
P2	Anthracene	550	10	13	0.13	2000
P3	Anthracene	550	10	88	0.88	13,200
P4	Anthracene	300	10	240	2.40	36,000
P5	Anthracene	350	10	250	2.50	38,000
P6	Anthracene	400	10	250	2.50	37,000
P7	Anthracene	450	10	170	1.70	26,200
P8	Anthracene	490	10	250	2.50	37,000
P9	Anthracene	550	10	200	2.00	30,000
P10	Anthracene	597	10	210	2.10	31,500
P11	Anthracene	460	1080	230	2.30	34,000
P12	Anthracene	502	960	230	2.30	34,000
P13	Biphenyl	301	10	180	1.80	27,100
P14	Biphenyl	460	10	190	1.90	28,000
P15	Biphenyl	602	10	210	2.10	31,500
P16	Anthracene (75%) Biphenyl (25%)	457	10	210	2.10	32,500
P17	Anthracene (25%) Biphenyl (75%)	479	10	190	1.90	28,000
P18	Anthracene (75%) Biphenyl (25%)	554	10	190	1.90	28,000
P19	Anthracene (90%) Ferrocene (10%)	453	10	220	2.20	33,000
P20	Anthracene (90%) SP-1 Fines (10%)	450	10	190	1.90	28,000

(A.E.I. (U.K.)) double-focussing, high resolution mass spectrometer. The essential features of this instrument which make it suitable for this study include,

- (1) ability to detect and identify materials of molecular weights up to about 1000;
- (2) high resolution allowing determination of molecular weights to a precision of about one in 50,000,
- (3) use of a heated probe to examine solids of low volatility and
- (4) rapid pump-out of sample ensuring low memory effects.

About 0.1 mg of sample was placed on the probe of the MS9 (temperature of probe 210°–250°C) and the spectrum run on U.V. photo-sensitised recording paper. Measurements of values of m/e and relative intensities were measured manually. Samples were

from freshly opened gold tubes, and include P1, P2, P4 and P7-P18.

2.4 X-ray analysis

To study the effect of pressure upon graphitisation, samples P1-P3, P7-P12, and P15 were subject to further heat treatment at atmospheric pressure, reaching 1000°C at 5°C min⁻¹, followed by heating to 2000° and/or 2800°C at rates of 10°C min⁻¹, and holding at the final temperature for 10 min. Heating was in an argon atmosphere using a graphite resistance furnace [14]. Extents of graphitisation were made from line-broadening measurements of the profiles of the (002), (004) and (110) X-ray diffractions. Samples were mixed and ground with 10 per cent of single-crystal silicon (Koch-Light Laboratories Ltd) to pass a 240 B.S. sieve and placed

in a 0.3 mm silica glass capillary (Pantak Ltd). X-ray powder photographs (57.4 mm radius camera, CoK_α radiation) were densitometered [15] to obtain the intensity profiles of the above diffractions. The crystallite size parameters L_c and L_a were obtained using the Scherrer–Warren approach [16]. Corrections were made only for instrumental broadening. No attempt is made to separate size-broadening from the strain-broadening component (see Warren–Averbach [17]). As a result little significance can be placed upon the absolute values assigned to L_c and L_a , but the direction of change and its relative magnitude is significant. Comparison with crystallite sizes determined in other laboratories is tenuous. The crystallite size L was obtained from the formula:

$$L = K\lambda/B \cos \theta$$

where λ = wavelength of X-ray
 θ = Bragg angle
 B = width of half-peak intensity (radians)
 K = 0.89 (002) (004) and 1.84 (110).

2.5 Optical micrographs

Stereoscan microscopy is limited to surface topography. Structural differences, e.g. isotropic and anisotropic constituents, are not detected. Recourse was therefore made to optical microscopy using reflected polarised light. Samples were mounted in Bakelite resin, surfaces initially ground and then polished with grades of alumina, and examined in a Carl Zeiss Standard Universal microscope, using partially crossed-polars and an oil-immersion with an Antiflex-Epi Zeiss objective lens. Images were recorded on Kodachrome IIA film from which were made black and white prints. Structural anisotropy was revealed by colour change, actual colour not being significant, isotropic material giving a continuous purple colour on rotation of the polariser.

3. RESULTS

3.1 Description of original and graphitised samples

P1 and P2, although both black in colour had a paste-like and a brittle structure respectively, with P3 being less brittle but more friable than P2. Samples P4–P5 were unchanged, P6 was purple compared to the white colour of P5, P7 was a black oily paste and P8–P10 black becoming progressively harder, P8 being malleable but not oily. P11 and P12 were essentially dry, black, soft solids. P13, P14 were of unreacted biphenyl, with P15 being a black dry brittle solid. P16 was an oily paste softer than P7; P17 was a loose brown powder and P18 was dry but paste-like. In contrast, P19 and P20 were dry black solids.

On further heat treatment it was the paste-like samples which subsequently fused with appreciable loss of volatiles i.e. P1, P7 and P11, see Table 2. The remaining samples did not fuse, pseudomorphs of the original sample being produced, often in high yield, e.g. P2, P3, P10 and P12.

3.2 Stereoscan micrographs

Selected micrographs are Figs. 2–13, and illustrate the development of quite a new phenomenon. Samples P1 and P2 (heated at the lower pressures of 13 MNm^{-2}) possessed a surface topography of little interest, comparable to that of P7 (Fig. 3), but on increasing the pressure at 550°C to the intermediate 88 MNm^{-2} (0.88 kbar) the micrographs revealed a structure composed almost entirely of spheres, P3 (Fig. 2) about μ -size. Most of these spheres were attached to other spheres at points of contact, and resembled a collection of pearls in a dish, or a bunch of grapes (the adjective botryoidal is used to describe such structures). Such structures were not observed at the lower temperatures of 300°C , 350° , 400° , and 450°C (P4–P7) at the upper pressure range used (about 200 MNm^{-2}). When P7 was subsequently

Table 2. Description and yields on further heat treatment

Code	Description	Yield, %		
		1000°C	2000°C	2800°C
P1	F	75	74	69
P2	P	96	95	94
P3	P	89	89	89
P7	F	57	50	47
P8	P	79	78	77
P9	P	93	88	86
P10	P			95
P11	F			86
P12	P			91
P15	P			62

F, fused and swollen to produce a sponge-like or frothy carbon.

P, pseudomorph produced; no swelling or fusing obvious.

heated to 2000°C (Fig. 4) signs of fusion are obvious. On increasing the temperature to 490°C at 250 MNm⁻² (2.50 kbar) the sample P8 exhibited discrete sub-units, not spheroidal in this case but rather elongated (spaghetti-shaped), (Figs. 5, 6), these sub-units retaining their characteristic shape on heating to 2800°C (Fig. 7). On further raising the temperature to 550°C at comparable pressures the botryoidal structure was again observed, (P9 shown in Fig. 8 and 9), but with spheres more perfect than those of P3. On heating P9 to 2800°C the sphere structure persisted but became rather more oblate and developed circumferential cleavage or shrinkage cracks (Fig. 10). The spheres are also seen in sample P10 (597°C at 210 MNm²) but there is evidence of coalescence of spheres (Fig. 11). On increasing the soaking time from 10 min to 16 hr at 500°C, the spaghetti-like structure did not disappear but grew somewhat larger (cf. P8 with P12, Fig. 6 and 12). The remaining samples possessed essentially featureless surfaces except Fig. 13 (sample P18) of the binary system, anthracene (75%)-biphenyl, from a fractured surface of which could be seen small protuberances. The graphite granules of P20 could also be seen. An electron diffraction examination of the spheres of P9

(2800°C) showed them to be polycrystalline and showing considerable preferred orientation.

3.3 Mass spectrometric analysis

The *m/e* values and intensities relative to anthracene (178) and biphenyl (154) are in Tables 3–6. Samples P4 and P13 are of non-carbonised anthracene and biphenyl respectively. During the ionisation process in the mass spectrometer and along the flight path of the ions and ion-radicals, certain new chemical species are produced. These are also observed in the carbonisation process and intensity corrections may be necessary. In making comparisons between the spectra and drawing conclusions from them, it is not possible to relate intensities of the spectra to concentrations in the original carbonisation sample. Molecular components have different vapour pressures at the probe temperature, and different efficiencies of ion-production. But comparisons of intensities of the same molecular species are valid provided these intensities are normalised relative to the same principal component, e.g. anthracene or biphenyl. Structural formulae of fifty-five component molecules which can be equated to given

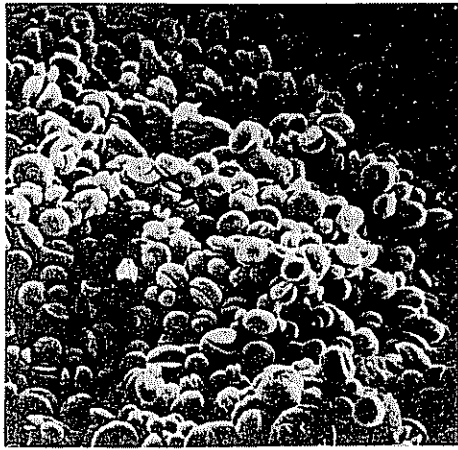


Fig. 10. Anthracene 550°C-2820°C
30,000 psi.
P9-CR3/62. 50μ



Fig. 11. Anthracene 597°C
31,500 psi.
P10-CR3/43. 50μ

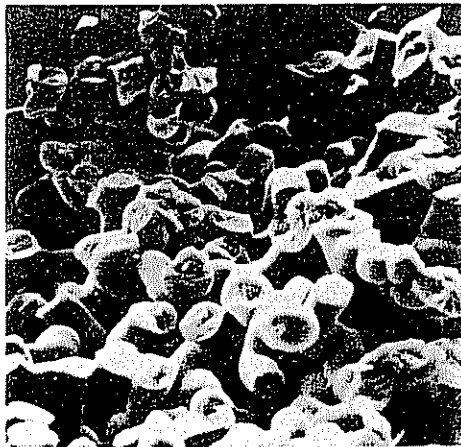


Fig. 12. Anthracene 502°C
34,000 psi. 16 hours.
P12-CR3/125. 50μ



Fig. 13. Anthracene 25%
Biphenyl 75%. 554°C
27,000 psi.
P18-CR3/51. 50μ

Figs. 10-13. 'Stereoscan' micrographs of surfaces of carbonised anthracene.

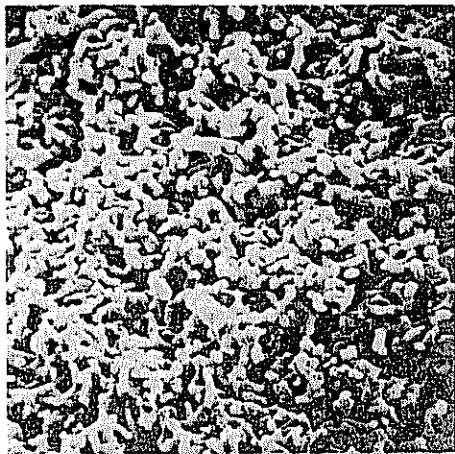


Fig. 6. Anthracene 490°C
37,000 psi.
P8-CR3/73.

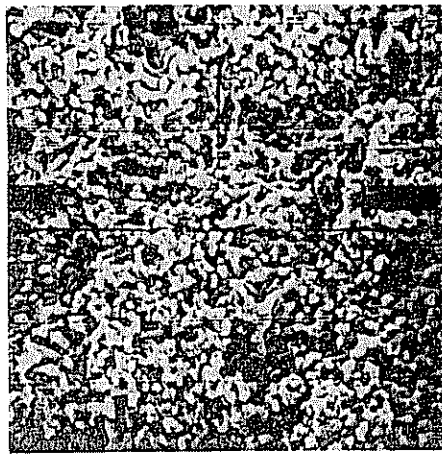


Fig. 7. Anthracene 490°C-2800°C
37,000 psi.
P8-CR3/140.

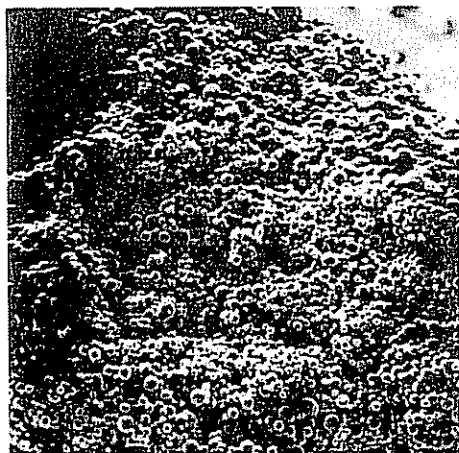


Fig. 8. Anthracene 550°C
30,000 psi.
P9-CR3/61.

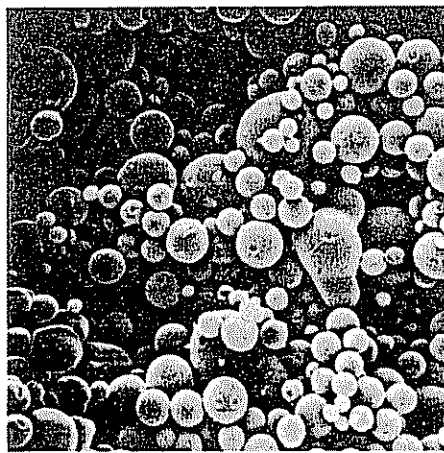


Fig. 9. Anthracene 550°C
30,000 psi.
P9-CR3/60.

Figs. 6-9. 'Stereoscan' micrographs of surfaces of carbonised anthracene.

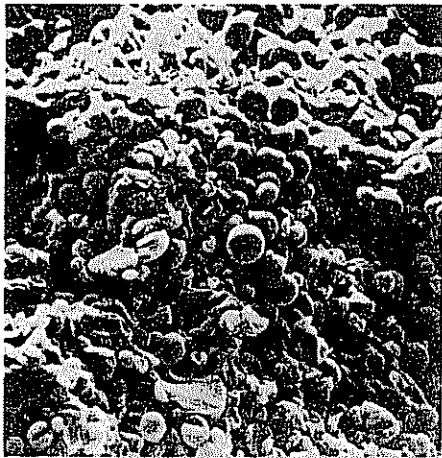


Fig.2. Anthracene 550°C
13,200 psi.
P3-CR3/101.



Fig.3. Anthracene 450°C
26,200 psi.
P7-CR3/69.



Fig.4. Anthracene 450°C-2020°C
26,200 psi.
P7-CR3/33.



Fig.5. Anthracene 490°C
37,000 psi.
P8-CR3/66.

Figs. 2-5. 'Stereoscan' micrographs of carbonised anthracene.



Fig.18. Anthracene 550°C
2,000 psi.
P2.

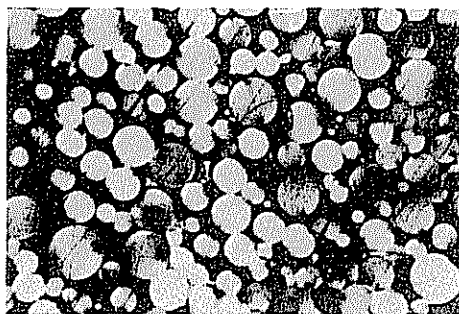


Fig.19. Anthracene 550°C
13,200 psi.
P3.

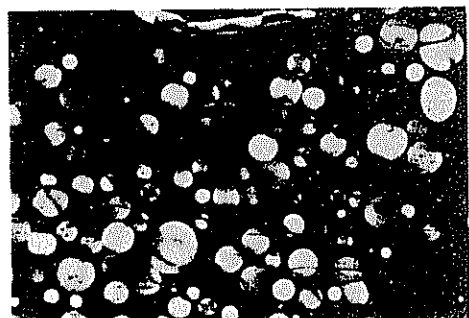


Fig.20. Anthracene 450°C
26,200 psi.
P7.

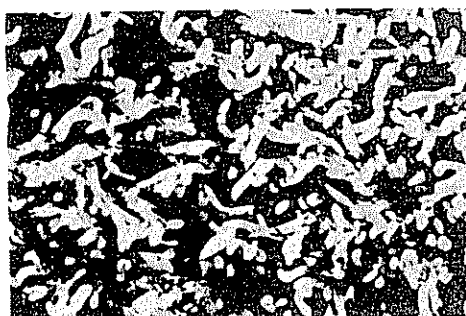


Fig.21. Anthracene 490°C
37,000 psi.
P8.

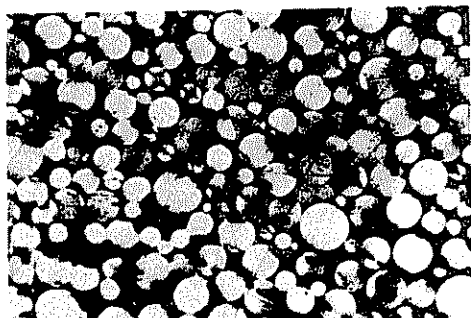


Fig.22. Anthracene 550°C
30,000 psi.
P9.



Fig.23. Anthracene 597°C
31,500 psi.
P10.

100 μ

Figs. 18-23. Optical micrographs of polished surfaces of carbonised anthracene and biphenyl, using polarised light.



Fig. 24. Anthracene 460°C
34,000 psi. 18 hours.
P11.

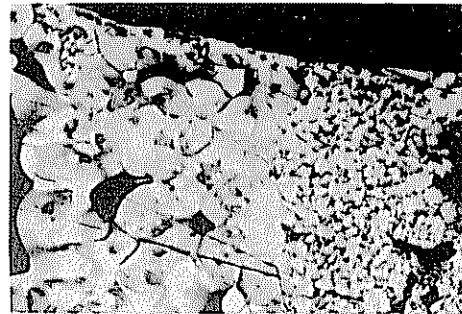


Fig. 25. Anthracene 502°C
34,000 psi. 16 hours.
P12.

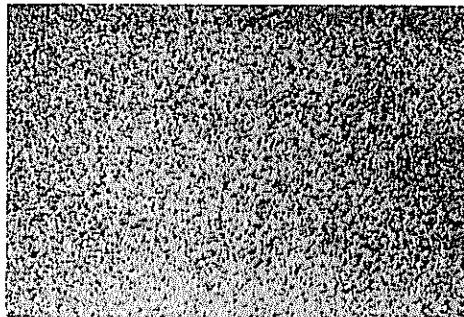


Fig. 26. Biphenyl 602°C
31,500 psi.
P15.

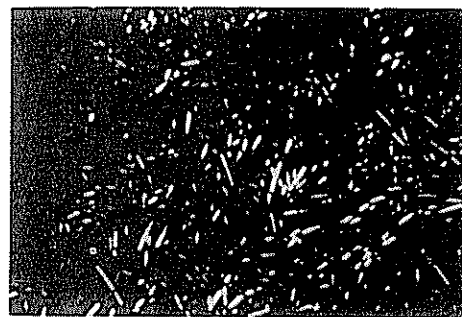


Fig. 27. Anthracene 25%
Biphenyl 75%. 554°C
27,400 psi.
P18.

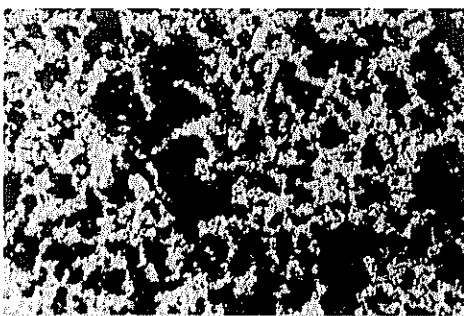


Fig. 28. Anthracene 90%.
Ferrocene 10%. 453°C
33,000 psi.
P19.



Fig. 29. Anthracene 90%.
SPI Fines 10%. 450°C
28,000 psi.
P20.

100μ

Figs. 24-29. Optical micrographs of polished surfaces of carbonised anthracene and biphenyl, using polarised light.

Table 3. Mass spectrometric data from carbonised samples

<i>m/e</i>	P4	P7	P8	P9	P10	Parent molecule
56	13	3	1	0	0	I
63	0.3	8	9	12	9	II
75	4	6	6	9	6	III
76	10	13	15	16	13	III
78	0.3	3	6	10	3	III
88	6	9	11	13	12	IV
89	10	15	16	15	15	IV
126	1.1	20	5	24	17	II
127	0.7	15	4	18	8	II
128	0.8	9	13	100	11	II
142	0.8	14	36	44	7	V
151	5.5	77	9	9	9	VI
152	5.0	44	10	11	14	VII
156	0.1	64	14	11	3	VIII
163	0.5	66	3	4	5	IX
164	0.2	52	8	4	28	IX
165	0.8	79	6	17	34	IX
176	13	95	15	16	20	IV
177	7	56	9	8	11	IV
178	100	100	100	100	100	IV
179	16	66	16	17	21	IV
180	1.3	33	5	4	11	IV
182	1.2	57	4	3	23	IV
191	0.6	31	12	24	36	X
192	0.8	23	18	41	67	X
202	0.5	18	6	30	54	XI or XII
204	0.3	8	2	12	33	XI
206	0.4	13	4	16	21	XIII
215	0.6	26	4	28	36	XIV or XV
216	0.3	0	3	25	40	XIV or XV
217	0.4	18	2	12	15	XVI
218	1.0	28	3	23	28	XVI
228	0.2	8	4	17	28	XVII
232	0.2	5	2	14	11	XVIII
242	0	0	1	9	0	XIX
252	0.1	26	6	46	15	XXI
254	0	6	2	35	17	XXI or XXII
263	0	20	1	4	0	XXIII
265	0	33	2	9	0	XXIII
266	0	28	2	15	0	XXIII
268	0	6	1	23	5	XXIV
274	0	10	2	0	0	
276	0	26	1	2	2	
278	0	28	1	3	0	XXV
280	0	26	1	4	0	XXVI
282	0	10	1	12	0	XXV or XXVI
289	0	40	1	1	0	XXVII
292	0	32	1	2	0	XXVIII
294	0	16	1	2	10	XXVIII or XXIX
296	0	6	1	2	2	XXVIII or XXIX

Table 3. (contd.)

<i>m/e</i>	P4	P7	P8	P9	P10	Parent molecule
302	0	98	5	2	10	VI
304	0	38	1	2	0	VII
306	0	42	1	1	0	VII
308	0	20	0.5	1	0	VII
316	0	139	0	0	0	XXX
318	0	70	3.3	1	0	XXXI
330	0	74	1	0	10	XXXII or IX
342	0	49	2	0	0	XXXIII
344	0	66	0	0	0	XXXIII
352	0	172	6	0	11	XXXIV
356	0	200	2	0	0	XXXV
358	0	197	0	0	0	XXXV
360	0	193	0	0	0	XXXV
374	0	44	0	0	4	XXXVI

m/e values are as in Figs. 14–17. No attempt is made to show structural isomers.

3.4 X-ray analysis

The results of the effect of pressure and other factors upon the graphitizability of anthracene and biphenyl, in terms of crystallite sizes L_c and L_a are listed in Table 7.

3.5 Optical micrographs

The original colour micrographs are reproduced in black and white, in Figs. 18–29. The essential findings from each specimen are as follows:

Sample P1. This was too soft to polish and dissolved in the mounting Bakelite resin. However, grinding produced some relatively smooth areas which revealed a total lack of anisotropy or anisotropic structures.

Sample P2 (Fig. 18). The surface was entirely anisotropic such as could have arisen from a complete coalescence of mesophase structures. There were isochromatic areas of considerable size. These results suggest that at the relatively low pressures of 13 MNm^{-2} (0.13 kbar) a mesophase may be identifiable at a temperature between 500° and 550°C .

Sample P3 (Fig. 19). The botryoidal structures prepared at 550°C and the intermediate

pressure of 88 MNm^{-2} (0.88 kbar) are essentially isochromatic apart from a colour change at the 'poles' of the sphere and as such are very comparable to the mesophase spheres described by Brooks and Taylor [1].

Samples P4–P6 could not be polished.

Sample P7 (Fig. 20). This shows clearly the formation of mesophase spheres from an isotropic matrix which is presumed to be a liquid at 450°C —the maximum, heat-treatment temperature. Anisotropic condensation occurs in the vicinity of the walls of the gold, containing tube. There is no indication of mesophase formation in the 'Stereoscan' photographs, suggesting that these spheres (Fig. 20) are still contained within the matrix of the material and do not appear on the surface.

Sample P8 (Fig. 21). This micrograph confirms the presence of the 'spaghetti' structure of the Stereoscan micrographs (Fig. 6, 7). The length of the rods are essentially isochromatic, indicating absence of strain or mis-orientation, but the head of the rod is often of a different colour so that growth is accompanied by some re-alignment. No isotropic or coalesced anisotropic phases were detectable.

Sample P9 (Fig. 22). The great majority of

Table 4. Mass spectrometric data from carbonised samples

<i>m/e</i>	P13	P14	P15	Parent molecule
76	16	10	24	III
77	8	5	12	III
78	2	1	3	III
89	1	1	9	IV
91	3	1	5	XXXVII
102	2	2	6	
115	4	4	14	XXXII
126	2	2	7	II
127	2	2	5	II
128	3	3	6	II
139	1	2	6	
152	24	22	40	XXXVIII
153	28	31	44	XXXVIII
154	100	100	100	XXXVIII
155	12	13	12	XXXVIII
165	2	1	36	XXXIX
167	4	1	30	XXXIX
168	0.6	0.4	40	XXXIX
178	0.5	0.3	24	IV
182	0	0	11	XXXVII
192	0	0	5	X
202	0.6	0.6	8	XI or XII
230	4	4	70	XL
244	1	0.4	18	XLI
252	0.5	0.5	5	XX
254	0	0	6	XXI
306	0.4	17	22	XLII
320	0	1	6	XLIII
330	0.2	0	3	XXXII
334	0.1	1	2	XLIV
344	0	0	1	XXXIII
382	0	0	6	XLV
396	0	0	2	XLVI
410	0	0	0.5	XLVII
458	0.6	0	0.2	XLVIII

this sample was made up of almost perfect spheres, of approximately equal size with a little coalesced anisotropic phase, showing actual growth of spheres into the condensed phase. On heating to 2800°C the spheres and coalesced phase show cleavage cracks, not dissimilar to those described by White, Dubois and Souillart[18]. The individual spheres lose their isochromatic appearance and appear speckled as crystallisation

within the sphere has re-orientated surface structure.

Sample P10 (Fig. 23). The botryoidal spheres are less frequent, somewhat larger and possess nodes (see Fig. 11). The optical microscope shows these larger spheres to result from coalescence of smaller units, there is much less isochromatism, and also that the phase formed from the coalescence of these larger spheres shows considerable misalignment or strain. There do not appear the polarised-light extinction contours of nodes and crosses, as observed by White *et al.*[18] suggesting that the structure of these spheres has enhanced lamellar alignment over the structures of White *et al.*

Sample P11 (Fig. 24). Although prepared at about the same temperature (460°C) as P7 (Fig. 20) the effect of increased soaking time is to remove entirely the isotropic phase and the mesophase to produce a coalesced phase possessing very considerable misalignment and strain. The extinction contours of White *et al.*[18] are much in evidence.

Sample P12 (Fig. 25) The effect of enhanced soaking time is to promote growth of the 'spaghetti' structure of P8 (Fig. 21) as also observed in the Stereoscan micrographs (Figs. 6, 12). But the preparation temperature of 502°C is probably too low to allow significant annealing in these larger structures of Fig. 25. The continuous, coalesced phase of P11 (Fig. 24) was quite absent.

Samples P13, P14 and P17 could not be polished.

Sample P15 (Fig. 26). The carbonised biphenyl (602°C) could be polished, no mesophase structures comparable to the anthracene were present, but although apparently totally isotropic, there were structures present, almost at the resolving power of the microscope, which exhibited anisotropic properties, changing colour or going from black to white. Heating to 2800°C enhanced the content of this second phase, but overall it still remained a minor component.

Table 5. Mass spectrometric data from carbonised samples

<i>m/e</i>	P16	P17	P18	Parent molecule
56	4	0	20	I
63	9	4	150	II
75	7	4	75	III
76	21	9	360	III
77	9	4	200	III
78	2	1	80	III
88	9	7	40	IV
89	19	0	70	IV
91	6	1	60	
92	1	1	15	
102	3	2	80	
115	10	4	190	
126	7	8	75	II
127	5	12	80	II
128	7	5	150	II
139	10	10	60	
142	30	3	25	V
151	15	24	190	VI or XXXVIII
152	24	19	600	VI or XXXVIII
153	36	40	800	XXXVIII
154	75	24	1250	XXXVIII
155	16	4	300	XXXVIII
156	4	2	25	VIII
163	19	25	25	IX or XXXII
164	13	18	25	IX or XXXII
165	45	40	190	IX, XXXII or XLIV
167	48	6	250	XLIV
168	16	1	300	XXXIX
176	40	18	25	IV
177	19	9	10	IV
178	100	100	100	IV
179	45	22	30	IV
180	22	47	25	IV
182	75	2	60	IV
191	15	4	10	X
192	20	3	10	X
196	14	0	10	
202	10	9	70	XI or XII
204	4	2	60	XIII
206	5	0	0	XIII
215	12	15	40	XIV or XV
216	6	3	15	XIV or XV
217	9	1	0	XVI
218	15	1	10	XVI
228	3	13	60	XVII
230	3	9	550	XL
242	2	1	10	XIX
244	2	1	50	XLI
252	9	5	0.6	XX or XXI
254	2	4	0.7	XXI

Table 5 (Contd.)

<i>m/e</i>	P16	P17	P18	Parent molecule
263	3	4	0	XXIII
265	7	4	0	XXIII
266	6	2	0	XXIII
268	2	2	0	XXIV
274	2	3	0	
276	6	8	0	
278	7	5	0	
280	5	1	0.7	XXV
282	2	0	0	XXV
289	8	18	0.3	
292	6	4	0	XLIX
294	4	3	0.5	XLIX
296	1	0	0	XLIX
302	10	16	0	VI
304	7	11	0	
306	15	275	4.5	XLII
308	3	66	0	XLII
316	21	9	0	XXX
318	12	4	0	XXXI
320	12	9	0.7	XLIII
330	36	220	0	XXXII
334	18	25	0	XLIV
342	13	0	0	XXXIII
344	12	6	0	XXXIII
352	57	2	0	XXXIV
354	25	2	0	L
356	42	2	0	L
358	34	2	0	XXXV
360	24	1	0	XXXV
382	2	1	0	XLV
396	1	0	0	XLVI
406			*	LI
428			*	LII
456			*	LIII
482			*	LIV
496			*	LV

*Just detectable.

Sample P16. This sample was almost entirely isotropic, but also present were small anisotropic components, larger than in Fig. 26 but quite difficult to photograph. The addition of the 25 per cent of biphenyl has completely altered the mesophase growth characteristics of P7 (Fig. 20) and P11 (Fig. 24).

Sample P18 (Fig. 27). There was a certain

resemblance to P16 but the anisotropic structures in the isotropic matrix were now larger and quite distinct. There is essentially a bi-phase system and it is possible that the small protruberances in the Stereoscan micrograph (Fig. 13) could be this anisotropic phase.

Sample P19 (Fig. 28). To anthracene was added 10 per cent of ferrocene and this

Table 6. Mass spectrometric data from carbonised samples

<i>m/e</i>	P1	P2	P11	P12	Parent molecule
128	4	6	8	32	II
142	4	0	42	7	V
154	5	3	0	5	XXXVIII
156	4	0.6	8	4	VIII
178	100	100	100	00	IV
192	19	30	11	12	X
202	2	6	2	5	XI or XII
206	4	6	4	5	XIII
216	2	3	4	5	XIV or XV
218	3	6	1	5	XVI
228	3	6	1	2	XVII
232	1	0	1	2	XVIII
242	3	0	0	2	XIX
252	3	0	3	12	XX
254	1	0	0	4	XXI or XXII
266	3	0	2	8	XXIII
268	1	0	1	1	XXIV
280	3	0	1	6	XXV
294	1	0	1	2	XXVIII
298	0	24	0	0	
302	5	15	5	72	VI
304	1	6	2	15	VII
306	1	0	1	5	VII or XLII
308	1	0	0	1	VII
316	5	21	1	30	XXX
330	2	9	6	24	XXXII
350	2	24	6	27	XXXIV
352	6	33	8	8	XXIV
354	3	48	9	9	L
366	1	33	14	7	
376	0	0	12	14	
382	0	0	8	13	XLV
386	0	0	6	4	XLVI
406	0	0	3	4	LI
418	0	0	5	2	
426	0	0	6	1	LII
428	0	0	6	1	LII
434	0	0	3	0	
456	0	0	2	0	LIII
470	0	0	4	0	LIII
484	0	0	3	0	LIII

figure shows a mesophase structure quite different from Fig. 20, or Fig. 24 (comparable preparation temperatures of 450°C). The ferrocene is exerting an influence here, the exact nature of which is not understood.

Evidently there is considerable scope for further investigation of the effect of addition of organometallic compounds.

Sample P20 (Fig. 29). The presence of the small graphite particles of the SP-1 material

Table 7. Crystallite sizes from X-ray line-broadening data

Sample	2000°C		2800°C		
	(002)	(004)	(002)	(004)	(110)
	L_c Å	L_c Å	L_c Å	L_c Å	L_a Å
P1	—	—	390	220	310
P2	380	160	650	630	5000
P3	350	150	790	450	3700
P7	140	120	730	350	5000
P8	190	140	1460	460	5000
P9	390	155	1500	480	4600
P10	—	—	1600	560	7000
P11	—	—	860	570	5000
P12	—	—	950	640	5000
P15	—	—	260	100	330

has apparently promoted mesophase coalescence as, at this preparation temperature of 450°C, no isotropic phase is detectable.

4. CONCLUSIONS

4.1 Growth of the botryoidal spheres

The development of discrete spherical structures, (Figs. 2, 8, 9, 19, 22) is a new phenomenon not previously reported. They appear to show considerable internal preferred orientation, but are randomly arranged relatively. The spheres retain their identity on graphitisation to produce a material which would exhibit isotropic bulk properties, but possess intrinsic anisotropic properties. The bulk density of such material could be controlled by compaction. Lowering the temperature of preparation from 550°C to 500°C produces, instead of spheres, rods or inter-connected 'spaghetti'-type units, with otherwise, similar properties to the spheres.

The growth mechanism of the isolated spheres is of interest. They could be the extended growth of the mesophase from the isotropic fluid, or they could result from a nucleation mechanism in a super-critical system enclosed in the bomb. In either case the individual spheres would grow freely

suspended in a hydrostatic pressure medium. The optical microscopy evidence suggests growth from the fluid phase. The observed structures arise from a rather unique situation created by a combination of temperature, soaking time and pressure, all three parameters promoting growth of the nematic liquid crystal type of structure and subsequent chemical condensation and increase in density (see Ref. [3]).

It would appear that at the pressures of 13 MNm⁻², mesophase growth and coalescence occur over a short temperature interval between 500° and 550°C (see Ref. [1]). Increasing the pressure enhanced molecular condensation reactions as well as the intrinsic viscosity of the system. Thus, at pressures of about 200 MNm⁻² at 450°C, the mesophase is still observable, the enhanced viscosity affecting both diffusion and coalescence rates. On further heating to 500° and 550°C, the isotropic liquid phase is entirely removed but the viscosity and surface tension of the spheres is such as to still prevent coalescence. At 600°C, the viscosity is reduced sufficiently to allow some coalescence. The creation of either rods (P8) or spheres (P3, P9) may depend upon temperature and soaking time. The entire phenomenon must therefore be attributed to a molecular system which

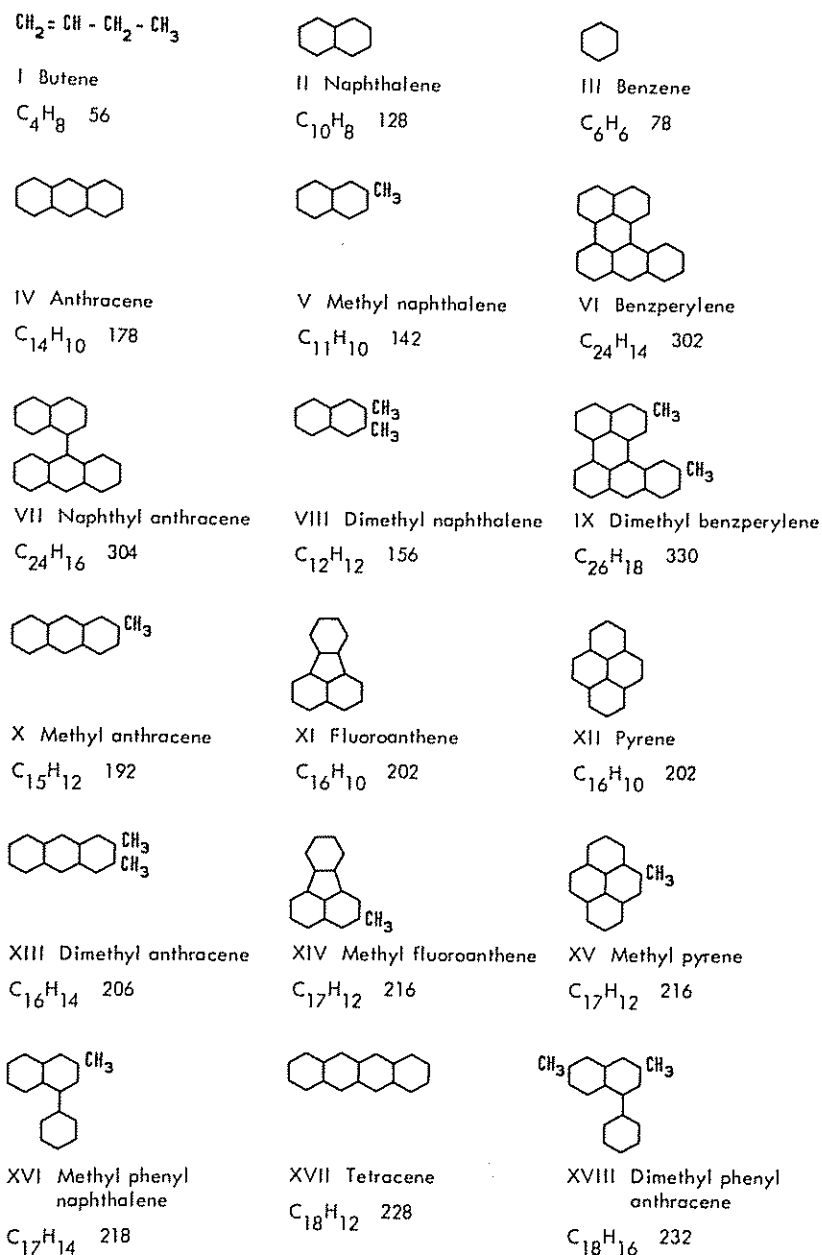


Fig. 14. Structural formulae of molecules identified in carbonised samples.

decomposes over a convenient temperature range to provide large lamellar molecules which can form the mesophase and have that specific viscosity at the requisite pressure

which does not allow coalescence until temperatures of semi-coke formation are reached. The mass spectrometric evidence supports the growth in size of molecules

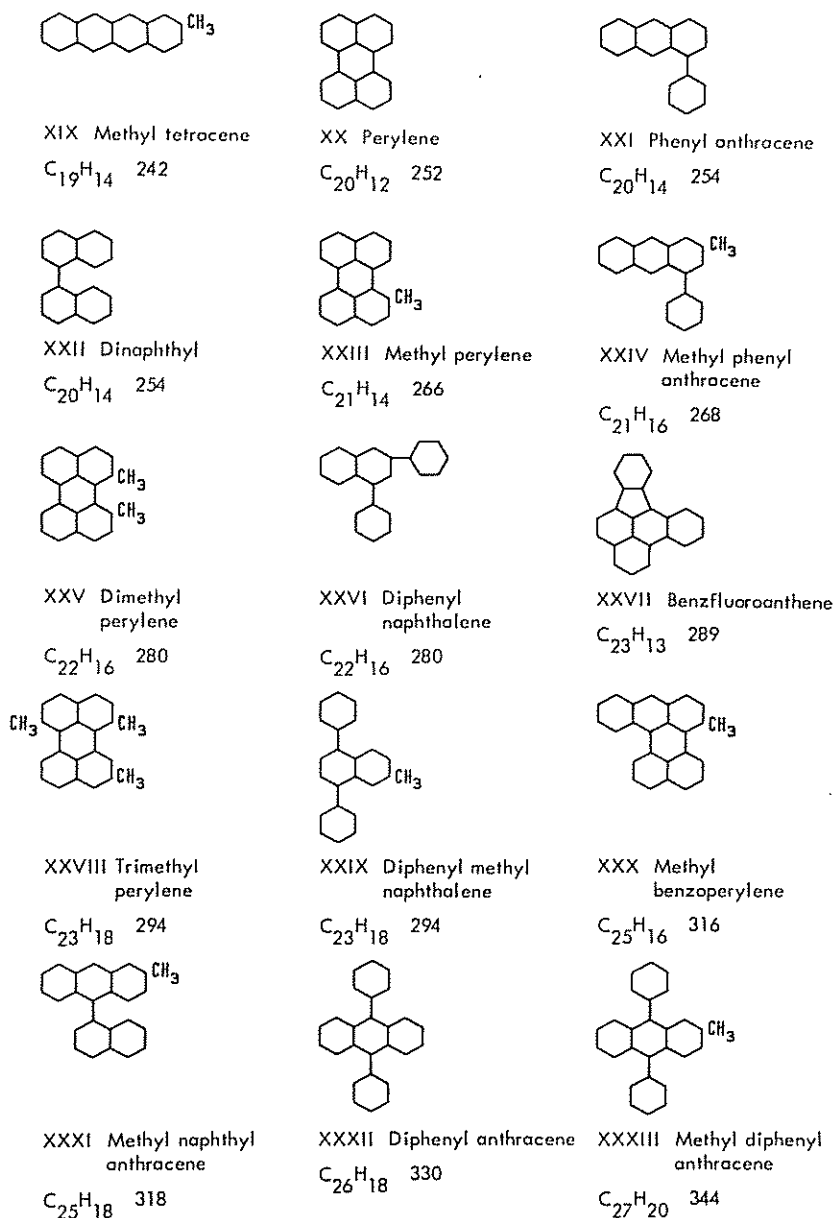


Fig. 15. Structural formulae of molecules identified in carbonised samples.

formed from anthracene to 550°C with little further reaction up to 600°C.

Brooks and Taylor[1] report the growth of the mesophase from large molecular weight material, e.g. isodibenzanthrone,

pyranthrone, naphthacene etc. This study has shown growth from the smaller anthracene molecule (178 a.m.u) confirming the report by Evans[6] for mesophase formation from acenaphthylene (152 a.m.u). Such

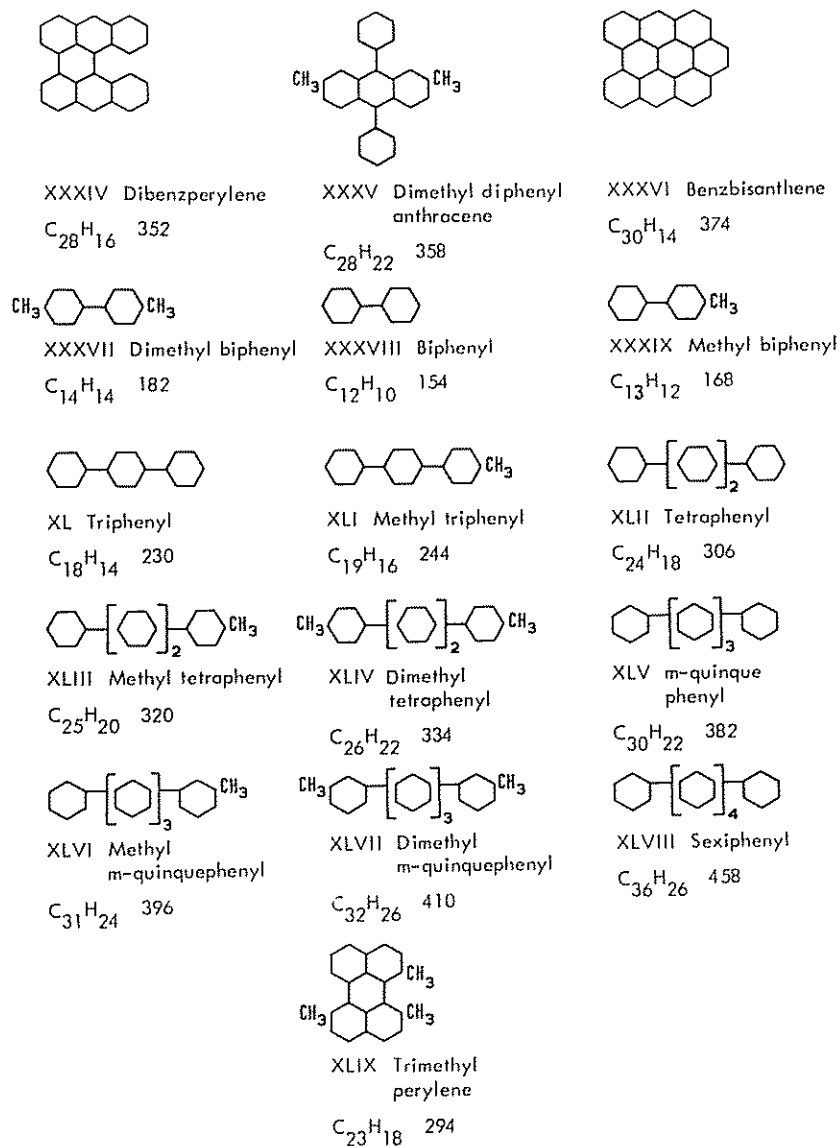


Fig. 16. Structural formulae of molecules identified in carbonised samples.

growth is therefore dependent upon the reacting molecule providing large lamellar products in a temperature range where fluidity and viscosity considerations are relevant.

These botryoidal structures seen in the Stereoscan and optical microscopes do resemble other reported structures, but their

properties and mode of formation are quite different. Commercial cokes made in 'bee-hive' ovens exhibited a 'herring-pore' or 'fish-roe' structure resembling a collection of pearls or beads. They are said to result from the thermal cracking of methane as distinct from acetylene, ethylene and ethane [19]. Brown *et al.*[20] report the formation of

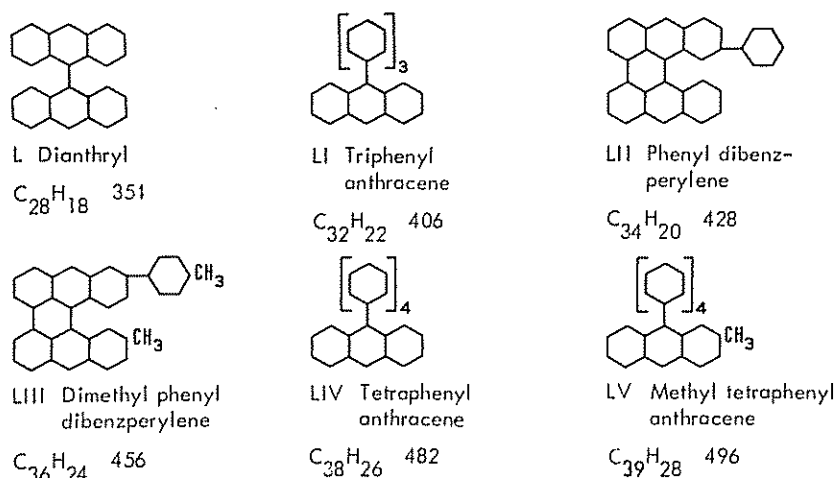


Fig. 17. Structural formulae of molecules identified in carbonised samples.

a spherulitic pyrolytic carbon from the cracking of tar vapours on high-temperature coke at temperatures above 700°C, but structure and mechanism of formation are quite different.

4.2 The X-ray analysis and effect of pressure

It would be unwise to place significance upon the actual values of L_c and L_a listed in Table 7, but correlations are possible.

Comparison of P1 with P8 shows that increasing the pressure of carbonisation from 13 to 250 MNm⁻² at 500°C considerably enhances the extent of graphitisation of the 2800°C sample; L_c (002) increases from 390 to 1460 Å, with L_a increasing from 310 to greater than 5000 Å. This is confirmed by comparison of P2 with P9 (550°C) where a similar increase in pressure increases the L_c of the 2800°C sample with P3, carbonised at an intermediate pressure (88 MNm⁻²), occupying an intermediate position. Evidently increasing the HTT enhances subsequent graphitisation. The effect of soaking time (comparison of P7, P8 and P11, P12) suggests that the increasing soaking time enhances subsequent graphitisation (cf. Ref. [3]). Heating P15 (biphenyl 602°C; 190 MNm⁻²) to 2800°C produces a product considerably more graphitic than that

reported by Walker and Weintraub[8]. This confirms the limited anisotropy seen in P15 by optical microscopy (Figs. 26, 27).

To summarise: increasing pressure, HTT and soaking time all contribute to enhanced graphitisation of the product subsequently heated under atmospheric pressure.

4.3 Carbonisation of Anthracene-Biphenyl mixtures—Mass spectrometric analysis

The mass spectrometer has provided information describing the molecular species produced during the carbonisation of anthracene and biphenyl under pressure and of any possible interactions between the anthracene and biphenyl. The following conclusions are drawn from the data of Tables 3–6.

Anthracene

Significant reactions of anthracene are ring breakage to produce C₄H₈ units, phenyl and methyl radicals and condensation of anthryl, naphthyl, phenyl and methyl radicals to produce molecules of progressively increasing size. Some thirty molecular species have been identified with intensities far exceeding those produced by pure anthracene. The greatest number of species appear in P7 (450°C) when the intensities,

and probably the concentrations of benzperylene (302, VI), dimethylbenzperylene or diphenylanthracene (330, IX or XXXII), methylated derivatives of IX and XXXII (344), methylbenzperylene (316, XXXI), dibenzperylene (352, XXXIV) and dimethyl diphenyl anthracene (358, XXXV) exceed the concentration of the remaining anthracene. On further heat treatment to higher temperatures (P8-P10), species of molecular weight above 260 tend to disappear, with a reappearance of material with molecular weight below 260.

Carbonisation at pressures of about 200 MNm^{-2} produces more molecular species than carbonisation at lower pressures (obtained from comparison with Evan's study [6]). In particular, more fragmentation of the anthracene molecule occurs resulting in quite extensive methylation and phenylation. Evans [6] also observed the rise and fall and subsequent rise in the number of molecular species with increasing HTT. This is attributed to initial fragmentation of the anthracene, subsequent condensation of the fragments, followed by the fragmentation of the smaller 'branched' species as condensation proceeds to produce molecules of molecular weight of several thousands. The effect of pressure is also to lower the temperature of fragmentation. For example, Evans [6] noted little decomposition on heating anthracene to 450°C . These considerations are very relevant in discussion of mechanism of formation of the botryoidal structures.

Many, if not all, carbonaceous materials on carbonisation produce carbons having ESR properties. The maximum free spin concentrations are of the order of 10^{19} per gram of carbon, associated with 1 per cent of all carbon atoms present. Likewise, to a first approximation, one molecule in every 100 molecules will possess the free electron. On examining the mass spectrographs for radicals these will only occur at very low levels of intensity if the radicals possess a diversity of structure. It is doubtful if they could ever

be found. But, if one radical structure is making a significant contribution to the ESR properties, then it could be located with a reasonable intensity. The major difficulty is one of distinguishing odd number m/e values of the radical from dehydrogenated products of molecules. In the samples of carbonised anthracene the m/e value of 289 occurred in P7, P16, P17. The intensity of the 289 peak was about 2 per cent of the sum of the intensity of all the peaks. The m/e of 289 is somewhat removed from materials of nearest molecular weight, e.g. diphenylnaphthalene 280, XXVI, trimethyl perylene, and diphenylmethylnaphthalene 294 (XXVII or XXIX). The structure of radical of mass 289, $\text{C}_{23}\text{H}_{13}$ could be XXVII. This radical could exist as such, or be bonded to a variety of structures giving it a range of thermal stability and accounting for the lack of fine resolution in the ESR signal (see, e.g. Ref. [21]).

Biphenyl

The biphenyl molecule is more stable than the anthracene (Table 4). On heating biphenyl to 460°C dimerisation was the principal reaction, but methylated tetraphenyl was also produced (320, XLIII and 334 XLIV). On heating to 602°C extensive ring breakage occurred to produce anthracene, naphthalene, and methyl and phenyl derivatives of these molecules as well as biphenyl, triphenyl, tetraphenyl and quinquephenyl.

Anthracene-Biphenyl mixtures

On heating to 450°C there is no direct evidence of co-condensation between anthracene and biphenyl. The amounts of phenyl anthracene correspond closely to those occurring when pure anthracene is carbonised (Table 5). Even in sample P17, with a large excess of biphenyl, the amount of diphenyl-anthracene corresponds very closely to the amount expected from the anthracene. On

heating P16 to 554°C the anthracene has evidently reacted leaving most of the biphenyl either unchanged, or as triphenyl. The formation of tetraphenyl appears to be restricted. Little or no phenylated anthracene is found, but this tends to disappear even in carbonised pure anthracene (Table 3). The overall conclusion appears to be that no phenylation of the anthracene appears to occur below 550°C and that beyond this temperature when the biphenyl may be more reactive, there is no anthracene remaining for reaction with the biphenyl.

Acknowledgements—One of us (H.M.) acknowledges the opportunity to study in Pennsylvania State University provided by P.I.W. and Professor Rustum Roy, the leave of absence from the University of Newcastle upon Tyne, and the support of Dr. G. W. Lee, O.B.E., Director of the British Coke Research Association, and Professor D. H. Whiffen, F.R.S., Honorary Director of the Northern Coke Research Laboratory. Financial assistance was provided from AEC grant AT(30-1)-1710.

We are grateful to Dr. H. E. Blayden and Dr. D. G. Edwards for discussions, Dr. D. G. Murchison for optical microscope facilities, to Mr. E. H. Boulton and Mr. P. Kelly for assistance with the Stereoscan and mass spectrometer respectively. This study forms part of the fundamental research programme of the British Coke Research Association, and we are grateful to the Council of the Association for permission to publish.

REFERENCES

- Brooks J. D. and Taylor G. H., *Chemistry and Physics of Carbon* (Edited by Philip L. Walker). Vol. 4, p. 243. Arnold, London (1968).
- Gray G. W., *Molecular Structure and the Properties of Liquid Crystals*. Academic Press, London (1962).
- Honda H., Kimura H., Sanada Y., Sugawara S. and Furuta T., *Carbon* **8**, 181 (1970).
- Weale K. E., *Chemical Reactions at High Pressures*. E. & F.N. Spon Ltd., London (1967).
- Griest E. M., Webb W. and Schiessler R. W., *J. Chem. Phys.* **29**, 711 (1958).
- Evans S., *A Mass Spectrometric Study of Carbonisation*, Ph.D. Thesis, University of Newcastle upon Tyne, England, December 1969.
- Evans S. and Marsh H., To be published.
- Walker P. L. and Weintraub A., *Proc. 3rd Conf. on Industrial Carbons and Graphite*, Society of Chemical Industry, London 1970, in press.
- Oberlin A., Rousseaux F. and Rouchy J. P., *J. Chim. Phys.* April Special Number, 160 (1969).
- Albert P., *J. Chim. Phys.* April Special Number, 171 (1969).
- Presland A. E. B. and Borah M. C., *Abs. 9th American Carbon Conf.*, Boston (1969).
- Thornton P. R., *Scanning Electron Microscopy*. Chapman & Hall, London (1967).
- Boulton E. H., *J. Sci. Inst. (J. Phys. E) Ser 2*, **1**, 565 (1968).
- Marsh H. and Wynne-Jones W. F. K., *J. Sci. Inst.* **42**, 710 (1965).
- Taylor A. B., *J. Sci. Inst.* **28**, 200 (1951).
- Warren B. E., *Phys. Rev.* **59**, 693 (1941).
- Warren B. E. and Averbach B. L., *J. Appl. Phys.* **21**, 595 (1950).
- White J. L., Dubois J. and Soullart C., *J. Chim. Phys.* April Special Number, 33 (1969).
- Simmersbach O., *Koks-Chemie*, p. 114. Springer, Berlin, (1914).
- Brown H. R., Hesp W. R. and Taylor G. H., *Carbon* **4**, 193 (1966).
- Jackson C. and Wynne-Jones W. F. K., *Carbon* **2**, 227 (1964).

